Terrain-aware three-dimensional radio-propagation model extension for NS-2

Sonja Filiposka and Dimitar Trajanov

SIMULATION published online 19 July 2010
DOI: 10.1177/0037549710374607

Simulation

Simulation: Transactions of the Society of Modeling and Simulation International
0(00) 1–17

DOI: 10.1177/0037549710374607
sim.sagepub.com
SAGE SCS

Terrain-aware three-dimensional radio-propagation model extension for NS-2

Sonja Filiposka and Dimitar Trajanov

Abstract

One of the weakest points of modeling wireless systems is radio-signal propagation in an irregular space. For that reason, it is essential that, when analyzing the performances of wireless networks, we observe the network in a natural three-dimensional terrain and we use an appropriate propagation model. However, care must be taken since such simulations demand extensive processing power, especially for mobile scenarios. In this paper, we present an extension for the NS-2 simulator with our optimized Durkin's propagation model based on digital elevation model data. Going one step further in creating a set of realistic simulation environments, we present a case study for modeling the behavior of a wireless *ad hoc* network via the social network of users grouped into scale-free communities. The case study presents a blend of topography responsive simulations with realistic traffic and movement pattern, while showing the numerous simulation possibilities of the presented extension.

Keywords

three-dimensional terrain data, Durkin's propagation model, *ad hoc* networks, communities, mobility, performances

1. Introduction

The ability to communicate with people on the move has evolved remarkably during the last decade. The mobile radio-communications industry has grown by orders of magnitude and made portable radio equipment smaller, cheaper and more reliable.[1] The large-scale deployment of affordable, easy-to-use radio-communication networks has created a trend of a demand for even greater freedom in the way people establish and use the wireless communication networks.[2]

One of the consequences of this ever-present demand is the rising popularity of *ad hoc* networks. A mobile wireless *ad hoc* network (MANET) is an infrastructureless network that can be established anywhere on the fly.[3] It consists of wireless mobile nodes that communicate directly without the use of any access point or base station. Thus, the nodes are supposed to establish a network environment by the means of self organization in a highly decentralized manner. In order to achieve this goal, every node has to support the so-called multihop paths. The multihop path concept is introduced to allow two distant nodes to communicate by means of intermediate nodes that graciously forward the packets to the next node closer to the destination. This is controlled by a special *ad hoc* routing protocol[4] that is concerned with discovery, maintenance and proper use of the multihop paths.

The independence of existing infrastructure, as well as the ability to be created instantly, that is, on demand, has made *ad hoc* networks a very convenient and irreplaceable tool for many on-the-go situations such as rescue teams on crash sites, vehicle to vehicle networks, lumber activities, portable headquarters, late-notice business meetings, military missions, and so on. Of course, every one of these applications demands a certain quality of service from the *ad hoc* network and usually the most relevant issues are the network performances in terms of end-to-end throughput.

Faculty of Electrical Engineering and Information Technologies, University Ss. Cyril and Methodius Karpos 2 bb, P.O. Box 574, 1000 Skopje, FYR Macedonia.

Corresponding author:
Sonja Filiposka, Faculty of Electrical Engineering and Information Technologies, Karpos 2 bb, P.O. Box 574, 1000 Skopje, FYR Macedonia.
Email: filipos@feit.ukim.edu.mk

However, the tradeoff of having no infrastructure and no centralized manner of functioning has influenced the *ad hoc* networks performances greatly in many aspects.

As for all wireless mobile communications, the mobile radio channel places fundamental limitations on the performances of the *ad hoc* network. Modeling the radio channel has historically been one of the most difficult parts of mobile radio-system design. Propagation models have traditionally focused on predicting the average received signal strength at a given distance from the transmitter, as well as the variability of the signal strength in close spatial proximity to a particular location. However, radio transmission in a mobile communications system often takes place over irregular terrain. Therefore, the terrain profile of a particular area needs to be taken into account when estimating the path loss since the transmission path between the transmitter and the receiver can vary from a simple line-of-sight (LOS) to one that is severely obstructed by buildings, hillsides, or foliage.

Typically, when estimating *ad hoc* network performances, very little attention is given to the terrain,[5] and thus, to the propagation model used for the estimation.[4,6,7] The nodes are assumed to be scattered on a flat, regular terrain and a simple ground-reflection propagation model is used. However, since terrain irregularities can greatly affect and distort the expected network performances, great care must be taken when trying to picture the real-life use of the modeled network.

In order to bring our observations a large step closer to real-life *ad hoc* network deployment, we decided to use a propagation model that incorporates the nature of propagation over irregular terrain and losses caused by obstacles in the radio path. We created an implementation of Durkin's model[8] as an extension for the NS-2 simulator,[9] thus allowing us to conduct more realistic simulation scenarios and analyze the way the terrain profile affects the *ad hoc* network performances.

Since the model is based on terrain information extracted from a Geographic Information System (GIS) file format, we also created a tool that can be used to create terrains in the given format by simple description of the terrain characteristics using a given number of triangular planes. In this way, we can model fairly simple, but also very rich, detailed terrains and avoid the necessity of using real-world data, since the appearance of the real-world data cannot be controlled in a satisfactory manner.

The rest of this paper is organized as follows. In section 2, the related work concerning terrain-aware radio-propagation models and implementations is given. Section 3 is an introduction to the digital elevation model (DEM) file format as well as a description of the tool we created for construction of artificial terrains that are described in this file format. Section 4 describes Durkin's irregular terrain propagation model and the way we implemented it in the NS-2 simulator. In section 5, case-study simulation scenarios are specified, while in section 6, the analysis of the performances of the case-study *ad hoc* network communities over three-dimensional (3D) terrains are presented. Finally, Section 7 concludes this paper.

2. Incorporating environment in wireless simulations

The field of terrain-aware radio-propagation models for wireless networks is a vibrant and popular field, especially in recent years. While the simulations conducted in the past were mainly occupied with statistically based propagation models that described the simulation environment on a large scale level with or without shadowing effects, lately the research community has shifted its interest to creation of a simulation scenario that will reflect real-life conditions as closely as possible.

There have been a number of different implementations of terrain-aware radio-propagation models, mostly in the form of a new framework for simulations. Examples typically include introducing a new realistic simulation framework, like the case for urban vehicle to vehicle networks,[10] wherein the authors developed this new simulation tool to evaluate the performance of event dissemination protocol in realistic city traffic environments.

Gunes and Wenig[11] made an attempt to combine realistic mobility models with obstacle models of radio propagation using a graph-based zone model. They used a ray-tracing approach for radio-wave propagation in an urban environment. The authors overcame the problem with time-consuming calculations when using ray tracing by feeding the NS-2 simulator with separately calculated ray-tracing data. However, it is assumed that radio signals are completely blocked by obstacles and a mobile node inside a building cannot communicate with a mobile node outside the building. Thus, the radio-propagation model used was very simplified.

Jardosh et al.[12] proposed a design of mobility and signal-propagation model for use in realistic network scenarios. The model allowed placement of obstacles that influenced the node mobility and the signal propagation. As for the signal-propagation model, which is the topic of our interest, the authors still used the two-ray ground-reflection model in combination with the free-space model, with the addition that the signal could propagate beyond obstacles, and the attenuation of the power of the signal when penetrating the obstacles was calculated.

Another interesting implementation is the AMADEOS extension[13] to NS-2 and Glomosim.[14] In addition to the developed mobility models, it provided a ray-tracing routine combined with a geometry DXF file that describes environment characteristics. The algorithm was based on a two-dimensional (2D) ray-tracing technique and was more than seven times slower than the two-ray ground simulations.

The OPNET's Terrain Modeling Module[15] added Earth topology, such as mountains, forests and valleys, as well as user-selectable environmental conditions to the simulated network model. There are several terrain-aware propagation models, which are included: the Longley–Rice model,[16] TIREM,[17] and the Walfisch–Ikegami model.[18]

We decided to follow the footsteps of OPNET and create an extension for the free open-source NS-2 that will provide the users with the ability to add terrains into their wireless scenarios. Durkin's model, which we have chosen for our implementation, works with DEM files in order to read in the profile data and is based on edge diffraction in a very similar approach to the one used by TIREM.

3. Terrain model

The GIS[19] integrates hardware, software and data for storing, management, analysis and representation of all forms of geographically referenced data. GIS technology[20] can be used for science purposes, cartography, urban planning, rescue missions and everywhere where need for geospatial parameters of the Earth's surface arises. GIS files are defined according to very strict standards for keeping record of digitalized data. GIS files contain elevation data, terrain shape, coordinate systems and projections, and one or more data that describe the precise shape of the Earth's surface according to the given coordinates.

The geographic systems are differentiated according to the way that they store the elevation data. There are two formats for data storing: raster and vector. The raster type of data consists of rows and columns of cells wherein a unique value is stored. Each cell gets a numeric value that can be represented by a unique identifier. The resolution of the raster data is the cell width and length in Earth units. Usually, the cells are square terrain areas, but other shapes can also be used.

The USGS DEM standard[21] is a geospatial file format developed by the United States Geological Survey (USGS) for storing raster-based DEMs. The USGS DEM file[22] is a set of ASCII coded blocks with a size of 1024 B. The file is organized in three categories of records labeled A, B and C.

Record A contains information for the origin and type of the terrain, as well as summary characteristics and measurement systems, which are used by the profiles. The profiles (records B) are columns with arbitrary length that contain raster elevations beginning at a certain location. Record C contains the standard deviation as quality-control data, as well as other statistics about the data precision.

3.1. Terrain generator

There are several software packets that allow the user to create an artificial terrain in the DEM file format, such as Terraform[23] and Terragen.[24] However, when using these applications, the user has no direct impact on the terrain shape, but as input parameters, the statistical characteristics of the desired terrain, such as the average height and the deviation from the average height in the sense of a global terrain contour (i.e. hill type or plain type), can be given. Our idea was to be able to give the precise shape of the desired terrain so as to completely control the outcome.

For these purposes, we developed a special tool for terrain generation. The tool provides terrain generation based on the input given by the user. The user needs to define the desired terrain by the means of a number of triangular planes. The input data for the terrain generator are the three coordinates of each triangular plane. The input is defined using an external XML file with the following specification:

```
<PLANE>
    <No.> </No.>
    <NAME> </NAME>
    <ENDPOINTS>
        <No.> </No.>
        <X> </X>
        <Y> </Y>
        <Z> </Z>
    </ENDPOINTS>
</PLANE>
```

The terrain is generated into a 7.5-minute DEM file, see Figure 1. The maximum and minimum heights of the terrain are calculated from the given input. The terrain data is stored relative to the minimum height. The resolution of the terrain is 10:10:0.1 (in m), as best given by the 7.5-minute standard.

Our artificial terrain generator allows us to create various types of terrains, from simple designed terrains consisting of several flat surfaces, up to rich detailed terrains that can closely resemble real-world terrain data. This possibility allows us to fine tune the simulation environment, that is, to create a terrain that perfectly fits the needs of the simulation. Thus, we gain more flexibility compared to real terrains for which you first need to find a terrain that has the wanted

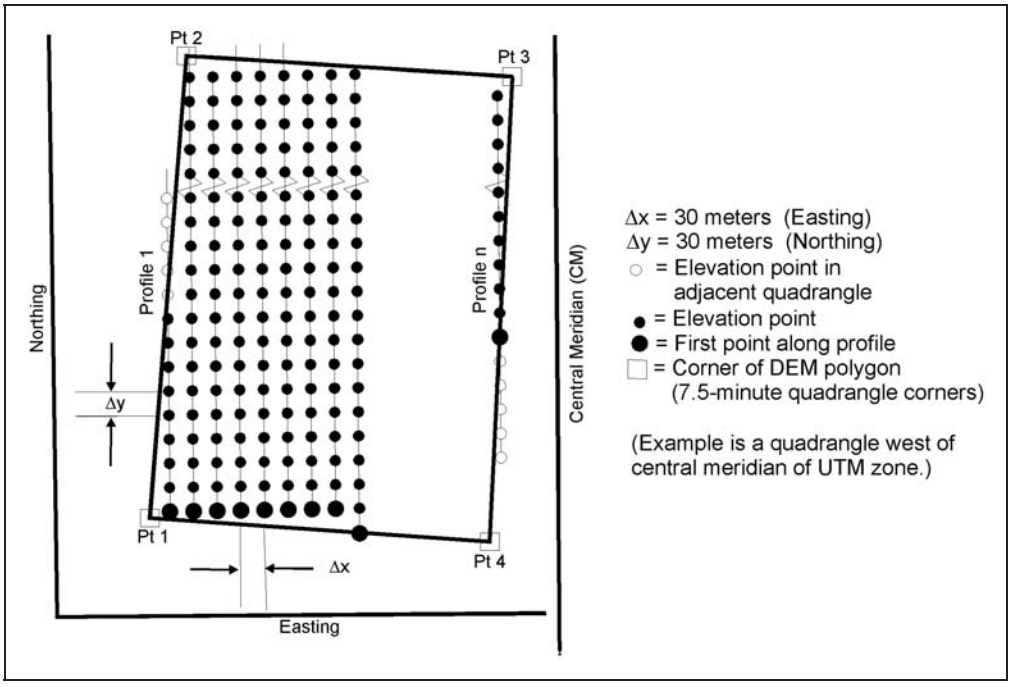

Figure 1. Extracting values for a 7.5-minute DEM file.

features and then cut it from the DEM file that contains it (the freely available DEM files are usually for very large areas) and create a new DEM file with the wanted piece, which is a time-consuming task. The terrain generator also creates the possibility of investigating exactly how much the terrain data influences the network performances when thinking in terms such as 'are the rough terrain features the ones responsible for the observed network behavior do or the small terrain discrepancies also play a big role in the shaping of the communication paths?'. This can be done by using a different level of details when generating the terrains for the simulations, and is one of our planned future steps in this study.

3.2. NS-2 nodes in three-dimensional space

Using our terrain generator, we are able to create various artificial terrains that can afterwards be read in the NS-2 simulator using the specialized DEM file class, which is already part of the NS-2 simulator. This class is one of the starting points for transition to 3D simulations. However, in the several last versions of this simulator, there is still no progress regarding the transition from 2D flat space to 3D space defined by the means of a DEM file. Using the existing class, which needed a few adjustments to work properly, we were able to read in a given DEM file and fill out the topographical database that will keep the terrain profiles needed for simulation. The topographical database can be thought of a 2D array. Each array element corresponds to a point in the simulated area map, while the actual contents of each array element are the elevation data.

The next step was to make adjustments in the way NS-2 treats the node coordinates, since, although when the classes were built it was thought to eventually transfer to 3D space, the functions always ignore the third coordinate for elevation. We redid the appropriate functions that were supposed to return the actual Z coordinate of the node in the 3D space by means of calculating the height of the ground level for the given X and Y coordinates of the node using the topographical database. With these changes, the NS-2 simulator was translated into 3D space.

Another fine adjustment was adding the possibility to regulate the scale of the terrain given in the DEM file. This is due to the fact that, if we decide to use real terrains, the ones that are publicly available on the Internet are usually very large, and thus not applicable for small- and medium-size wireless network simulations. Our solution offers the user to read in a DEM file that describes a large terrain and then scale it to a desired size inputted by the user in the tcl script that describes the simulation scenario. In the input tcl script that describes the simulation scenario, the desired width and length of the terrain is given. Using these values, after reading in the given DEM file, we scale the data using the new values for terrain dimensions. This feature also allows us to make the resolution of our terrain

much higher than the 10:10:0.1, as given by the standard. Thus, the accuracy can be set to 1 m or even less.

4. Durkin's propagation model

When simulating wireless mobile networks habitually, we come to use one of the large-scale propagation models that estimate the radio-coverage area of a transmitter for an arbitrary transmitter–receiver separation distance.[25] These practical and fast, yet terrain-unaware, frequently used propagation models available in NS-2 are the free-space propagation model or the ground-reflection (two-ray) propagation model.

The free-space propagation model is used to predict received signal strength when the transmitter and receiver (T–R) have a clear, unobstructed LOS path between them. In a mobile radio channel, a single direct path between T–R is seldom the only physical means for propagation, and hence the free-space propagation model is, in most cases, inaccurate when used alone. The two-ray ground-reflection model is a useful propagation model that is based on geometric optics, and considers both the direct path and a ground-reflected propagation path between T–R. This model has been found to be reasonably accurate for LOS microcell channels. At large distances, the received power falls off with a rate of 40 dB/decade. This is a much more rapid path loss than is experienced in free space. However, please note that this model does not depend on the radio frequency used for transmission.

One of the basic mechanisms of radio propagation is diffraction, which causes radio-signal distortions. Diffraction allows radio signals to propagate around the curved surface of the Earth and to propagate behind obstructions. The concept of diffraction loss as a function of the path difference around an obstruction is explained by Fresnel zones. Fresnel zones represent successive regions that have the effect of alternately providing constructive and destructive interference to the total received signal. In mobile communication systems, diffraction loss occurs from the blockage of secondary waves such that only a portion of the energy is diffracted around an obstacle. That is, an obstruction causes a blockage of energy from some of the Fresnel zones, thus allowing only some of the transmitted energy to reach the receiver. Depending on the geometry of the obstruction, the received energy will be a vector sum of the energy contribution from all unobstructed Fresnel zones.

When shadowing is caused by a single object, such as a hill or mountain, the attenuation caused by diffraction can be estimated by treating the obstruction as a diffracting knife edge. This is the simplest of diffraction models, and the diffraction loss in this case can be readily estimated using the classical Fresnel solution for the field behind a knife edge. The diffraction gain due to the presence of a knife edge, as compared to the free space, is given by

$$G_{\mathrm{d}}(\mathrm{dB}) = 20\log\left|F(v)\right| \tag{1}$$

where $F(v)$ is the Fresnel integral, a function of the Fresnel–Kirchoff diffraction parameter v, defined as

$$v = h\sqrt{\frac{2(d_1 + d_2)}{\lambda d_1 d_2}} \tag{2}$$

where h is the relative height of the obstruction, d_1 and d_2 are distanced from the obstacle to the transmitter and the receiver, respectively, and λ is the radio-signal wavelength. In practice, graphical or numerical solutions are relied upon to compute the diffraction gain. An approximate solution for (1) provided by Lee[26] is

$$\begin{array}{cc}
G_{\mathrm{d}}(\mathrm{dB}) = 0 & v \le -1 \\
G_{\mathrm{d}}(\mathrm{dB}) = 20\log(0.5 - 0.62v) & -1 \le v \le 0 \\
G_{\mathrm{d}}(\mathrm{dB}) = 20\log(0.5e^{-0.95v}) & 0 \le v \le 1 \\
G_{\mathrm{d}}(\mathrm{dB}) = 20\log\left(0.4 - \sqrt{0.1184 - (0.38 - 0.1v)^2}\right) & 1 \le v \le 2.4 \\
G_{\mathrm{d}}(\mathrm{dB}) = 20\log\left(\frac{0225}{v}\right) & v > 2.4.
\end{array} \tag{3}$$

4.1. Durkin's model

The median transmission loss predicted using the path geometry of the terrain profile is the goal of Edwards and Durkin,[8] as well as Dadson.[27] Our implementation of this propagation model in the NS-2 working environment closely follows their concepts.

The execution of the path-loss estimation consists of two parts. The first part addresses a topographic DEM file turned into a topographical database (see section 2) and reconstructs the ground-profile information along the path between T–R. The second part of the algorithm calculates the expected path loss along that path.

Specifically, we move along the line that connects T–R in discrete steps. The width of the step can be adjusted by the user; the default is 1 m. In each step, we check for LOS over the T–R line and then, with the same step size, we move vertically or horizontally (above and below, or to the left and to the right, respectively) checking the clearance of the first Fresnel zone in 3D space. This means that we consider potential penetration of the Fresnel zone, not only in the Z plane along the T–R line, but also in its 'sides', see Figure 2. This additional 3D observation is not done in the original Durkin model.

At this point, the algorithm must make decisions as to what the expected transmission loss should be. The first step is to decide whether a LOS path exists between T–R. The LOS condition is violated whenever there is an obstacle higher than the T–R line. The LOS check is done only along the T–R line, and the obstacles found in the rest of the Fresnel zone have no impact on the LOS path.

The second part of the algorithm is checking to see whether first Fresnel zone clearance is achieved. If the Fresnel zone of the radio path is found to be unobstructed, then the resulting loss mechanism is approximately that of free space. In each step along the T–R line and inside the first Fresnel zone, we compute the difference between the height of the line joining T–R antennas and the height of the ground profile in the given cell in 3D space. The method for determining first Fresnel zone clearance is done by first calculating the Fresnel diffraction parameter v, defined in (2), for each of the j ground elements.

According to the original Durkin model, if $v_j \leq -0.8$ for all $j = 1, \ldots, n$, then there is no additional loss due to diffraction. For this case, the received power is calculated using the plane Earth propagation. If the terrain profile failed the first Fresnel zone test (i.e. any $v_j > -0.8$), then there are two possibilities: non-LOS or LOS, but with inadequate first Fresnel zone clearance.

For both of these cases, the algorithm calculates the free-space power and the received power using the plane Earth propagation equation. The algorithm then selects the smaller of the powers as the appropriate received power for the terrain profile. If the profile is LOS with inadequate first Fresnel zone clearance, there is loss that is added (in dB) to the appropriate received power. This additional diffraction loss is calculated by (3).

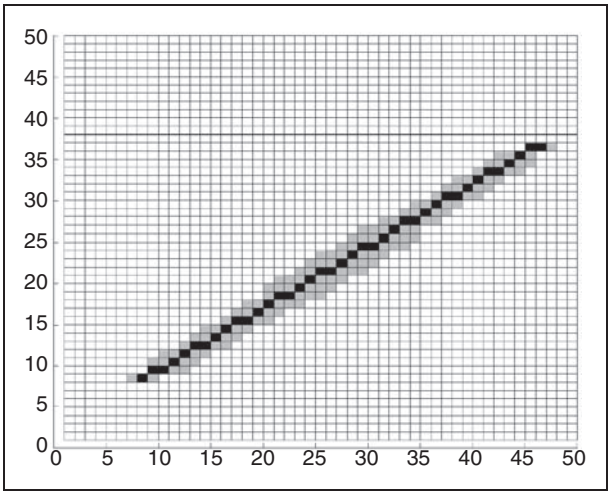

Figure 2. Range of cells of the topographical database that are investigated for an example T–R pair.

The loss is evaluated using the highest value of the diffraction parameter v, which means that we settle for the worst case of all existing diffraction knife edges. For the case of non-LOS, the system grades the problem into the category of single diffraction edge. This is a first step simplification of the procedure that, in the future version of the software, we intend to expand and correct so that we check for two, three and more diffraction edges using the Epstein and Peterson method.[28]

4.2. Durkin model implementation in NS-2

In order to apply Durkin's model in the NS-2 simulation environment, we created a new type of propagation model, Durkin, which is based on the previously described algorithm.

The antenna height (in 3D space), the carrier frequency of the radio signals and node position in 3D space are input parameters to the propagation model. The overall node elevation is the sum of terrain elevation and antenna height.

As explained earlier, if the first Fresnel zone of the radio path is unobstructed, the expected signal-loss calculation is according to the free-space propagation model. At the moment of loss of LOS or breach of the Fresnel zone, the procedure calculates the loss due to the diffraction losses. For our first set of investigations, we settled for single knife-edge diffraction in order to lessen the computational burden that was introduced to the simulator.

We also had to modify the CSMA/CA (Carrier Sense Multiple Access with Collision Avoidance) channel in NS-2 so that it can determine the presence of the terrain, i.e. LOS. The current design of the NS-2 wireless channel considers square shape of the physical carrier sense range of the transmitting node. Hence, the nodes that are in the range of that square are not able to access the channel. Using our propagation model results in physical carrier sensing ranges of the transmitting node, similar to its real-world omni-directional spherical shape when there are no obstructions near the node.

Nevertheless, the transmission and physical carrier sensing ranges of the signal propagation of the nodes are not ideal circles, but they depend on the terrain configuration. The situation without terrain assumes that some nodes might be blocked by other sending nodes, for example the hidden and exposed terminal problems. Considering the terrain as another parameter implies that some obstacles might limit the interferences between the nodes. In this way, the resources of the channel are more utilized and the hidden and exposed terminal problems are reduced.

While implementing Durkin's propagation model in NS-2, one of the goals was to make it as close to the

two-ray ground model as possible when considering a completely flat terrain described with a DEM file. In order to do this, there are several implications that must be taken into consideration. First, as we noted previously, the two-ray ground model does not include the frequency of the radio signal, while for Durkin's model, this value is needed in the final calculations of the received power, diffraction parameter and loss. Thus, one must not overlook the need to set the frequency to 2.4 GHz when simulating the wireless network according to the 802.11b/g standard. This must be done in the tcl script that defines the simulation, since the default frequency used in the NS-2 simulator is 914 MHz, which will lead to completely different results. Here, we must point out that Durkin's extension is not restricted to the use of 802.11 networks. It is made as a standalone radio-propagation model, and can be used for any wireless network as long as the necessary parameters are set to their appropriate values according to the network type.

The NS-2 simulator has three threshold values that define whether the received signal causes interference or not (this is the carrier sense threshold value $\text{CSThresh} = 1.559 \times 10^{-11}$), whether it can be received and recognized as a packet or not (this is the d received power threshold $\text{RXThresh} = 3.652 \times 10^{-10}$), and whether there is a packet collision or not (this is the signal to interference ratio, $\text{SIR} = 10$).[29] When using these values in combination with an antenna height of 1.5 m (this is the default value for the height of the antenna of the node), the two-ray ground model provides signal power above the received power threshold for distances below 250 m, while the interference range is up to 550 m. These ranges are consistent with the IEEE 802.11b standard.

In order to have the same range of 250 m and 550 m for receiving and interference regions, respectively, when using Durkin's model with a regular flat terrain, some modifications are needed. This is due to the fact that when the T–R distance is above 72 m, part of the first Fresnel zone is starting to hit the ground, thus creating a breach of the zone, which implies loss and lowering of the power level computed according to the two-ray ground model. Because for distances above 350 m, the diffraction parameter becomes less than -0.8, the loss in these cases is 0 according to the original Durkin model. However, this is not the case if we follow (3), where the value of the diffraction parameter needs to be below -1 for no-loss conditions. Since we wanted to keep the limit of 550 m as an interference range, in our implementation we adopted Durkin's proposition of -0.8 as a border value for the diffraction parameter. As for the 250 m range, because of the additional loss, the received power threshold value must be changed to 2.9996×10^{-10}, which can be done in the tcl script. In this way, the receiving and interference range are the same as the ones for the two-ray ground model.

As for the third parameter that is used when deciding for collision of packets, we made no changes. This means that when several packets arrive at the node, the power ratio should be at least 10 for the algorithm to decide that there is no collision. Because the rate with which the radio signal decreases with increasing distance is different for the two-ray ground model and Durkin's model for flat terrain, the number of collisions will be different, and using Durkin's model, the simulator may decide on a greater number of collisions compared to the two-ray ground model. However, we found that this does not significantly influence the obtained results.

In Figure 3, the obtained results for the ratio of the received and sent packets when using the two-ray ground model and Durkin's propagation model with a perfectly flat terrain are presented. Since we took care to set the threshold values to the corresponding levels, the effect of the signal to interference ratio is shown with the discrepancy in the obtained results. It can be seen that for larger offered load when the number of packets that is considered rises, the difference between the two models diminishes to 1% or 0%. The highest difference is visible for static nodes since, in this case, the positioning of the nodes is constant and the collisions are ever present. However, the maximum difference is not higher than 15%.

Our first implementation of Durkin's model[30] has proven to be very slow when trying to simulate mobile networks, and has been redesigned and optimized in order to provide a much faster estimation of the received power. The main reason for optimization was the overwhelming number of times the algorithm

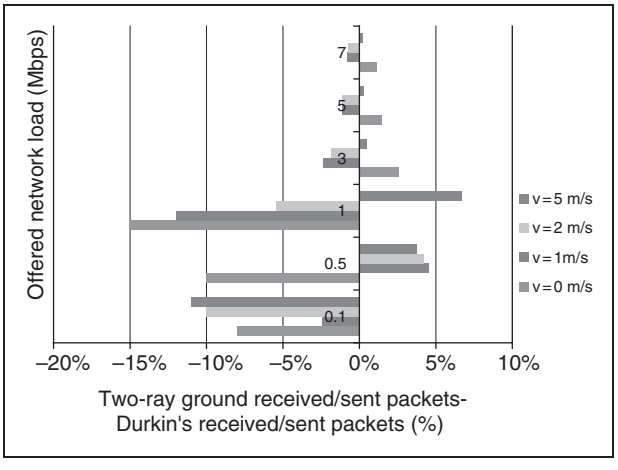

Figure 3. Performance comparison of the two-ray ground model and Durkin's propagation model for a perfectly flat terrain and random traffic and movement.

needed to access the topographical database. By means of a software profiling tool, we analyzed the performances of our new class for Durkin's propagation model, and found that the repeated accessing to the topographic database, which is held in memory as a dynamic one-dimensional array, is the most time-consuming part because it is a function call that is used around 10 times more than any other call in the algorithm. This behavior was due to the large amount of interpolations carried out for points inside the Fresnel zone. In this way, we noticed that a great part of the area of the first Fresnel zone is checked more than once, which is, of course, not necessary. In order to optimize the code, in our new version, we do not compute any interpolations between the neighbor values of the topographical database. This does not reduce the quality of the results since, apart from the original Durkin implementation, we not only check the elevations along the T–R line, but also check the complete first Fresnel zone, which again spreads over the neighboring cells. An example of the range of the topographical database that is investigated in order to decide upon a single T–R pair is given in Figure 2.

In addition, the other calculations mainly consist of time-consuming functions such as square roots and logarithms, which also add to the time needed for processing one pair of transmitting receiving nodes. When taking into consideration that in NS-2, this is done in a way that, for each transmitting node, the receiving power level at every other node that is part of the network has to be calculated in order to decide whether there is interference or not, we came across a performance problem, as the simulations were taking a tremendous amount of time.

In order to lessen the computing time, at the beginning we discard the 'impossible' situations, that is we immediately calculate the receiving power according to the free-space propagation model, and if it is below the interference threshold, we do not need to check whether the signal is even less stronger than our first-order optimistic approximation. In addition, whenever the diffraction parameter reaches its 'highest' value of 2.4, according to (2), we no longer need to search for another knife edge since the one encountered is 'bad enough'.

Another performance enhancement is introducing a cache in the case of simulation of static nodes. Since, for static simulations, the once already calculated received powers for a given transmitter cannot change, we decided to keep these values in a cache in a form of an $N \times N$ matrix, where N is the number of nodes in the simulation. At the beginning of the algorithm, we first check to see whether we already have the necessary values in the cache. If they are available, we simply reuse them, otherwise we calculate and add the new values in the cache. In this way, the speed of completing our simulation sets was brought back to the original when simulating in the usual 2D environment.

As for the cases of mobile nodes, the careful code optimizing by reducing the call of the topographical database to the minimum and by reducing the number of time-consuming complex calculations, i.e. the square root whenever calculating the distance between two points, has proven to be satisfactory. The optimized Durkin propagation model for NS-2 now runs with a speed that is comparable to the popular two-ray ground model.

Figure 4 allows for a comparison of the average time of execution of the different simulation sets for various node speeds when using the different propagation models. The results clearly show that, even for the worst case scenario of flat terrain, when using Durkin's propagation model, the average time of execution of the simulation scripts is not significantly different when compared to the two-ray ground model. In this way, we show that the price of creating a more realistic scenario is very small and yet leads to more significant results. The total computation time spent on simulation of the L = RND P = RND scenarios using the two-ray ground-propagation model was almost 83 hours, while using Durkin's propagation model with a perfectly flat terrain, it was almost 98 hours, which results in only 18% more computation time spent. Here, we must note that the values shown largely depend upon the type of simulation, since the execution time is very dependent upon the size of the trace file, given that the task of writing to disk is the most time-consuming part, and very much depends on the number of packets that flow through the network and on the level of tracing.

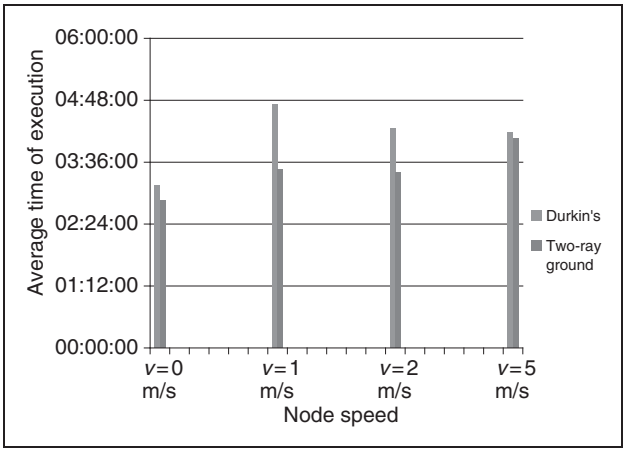

Figure 4. Average time of execution comparison of the two-ray ground and Durkin's propagation model for a perfectly flat terrain and random traffic and movement.

4.3. Verification of Durkin's model implementation

Since there are numerous freely available tools for radio-propagation analysis that incorporate the Longley–Rice propagation model, and this model is also available in the OPNET simulator, we decided to verify our implementation of Durkin's radio-propagation model by comparing the radio coverage we obtain with the one that would be given by the Longley–Rice model for the same terrain and position of the transmitter. This model is not as detailed as the TIREM model, but is freely available compared to the proprietary TIREM model.

The Longley–Rice model,[16] also known as the Irregular Terrain Model (ITM), is a radio-propagation model usable within a frequency range of between 20 MHz and 20 GHz. The Longley–Rice model considers any influences of the following parameters: distance between transmitter and receiver, antenna altitudes, channel frequency, terrain profile, ground refraction, ground-surface impedance and types of climate circumstances.

The ITM model has two modes: area and point-to-point (PTP) mode. Area mode is used in cases where the exact terrain is not known. Environmental parameters and statistical parameters are used in calculating path loss. Terrain roughness is approximated from a user-entered value that represents the change in terrain height. When using PTP mode, the model retrieves a terrain profile based on the user entered latitude and longitude values for the transmitter and receiver. Statistical and environmental parameters are used with the terrain profile in calculating path loss. The PTP model relates the statistical variance of terrain elevations to classical diffraction theory, and predictions made by the model agree with measured data. While other prediction models construct approximations to the terrain as combinations of classical diffraction edges, the PTP model constructs an equivalent rounded obstacle in terms of terrain elevation statistics.

For our verification purposes, we used the ITM model as implemented in the point-to-point mode in the widely popular freely available tool for radio links prediction Radio Mobile.[31] All of the parameters in the application were set to correspond to the values used in the NS-2 simulator. We made a number of comparisons with several different real terrains, and the obtained results differed to the case shown here by up to a maximum of 5%. Here, we present one characteristic example of our verification comparisons. As shown in Figure 5, we observed the radio coverage given both the ITM and Durkin models of a given location of a transmitter in a real terrain (the terrain used is shown in Figure 7). Figure 5 presents the radio coverage calculated with the ITM model (left) and with Durkin's model (middle). No scale for the signal is given since the NS-2 simulator does not have need for its value; it only

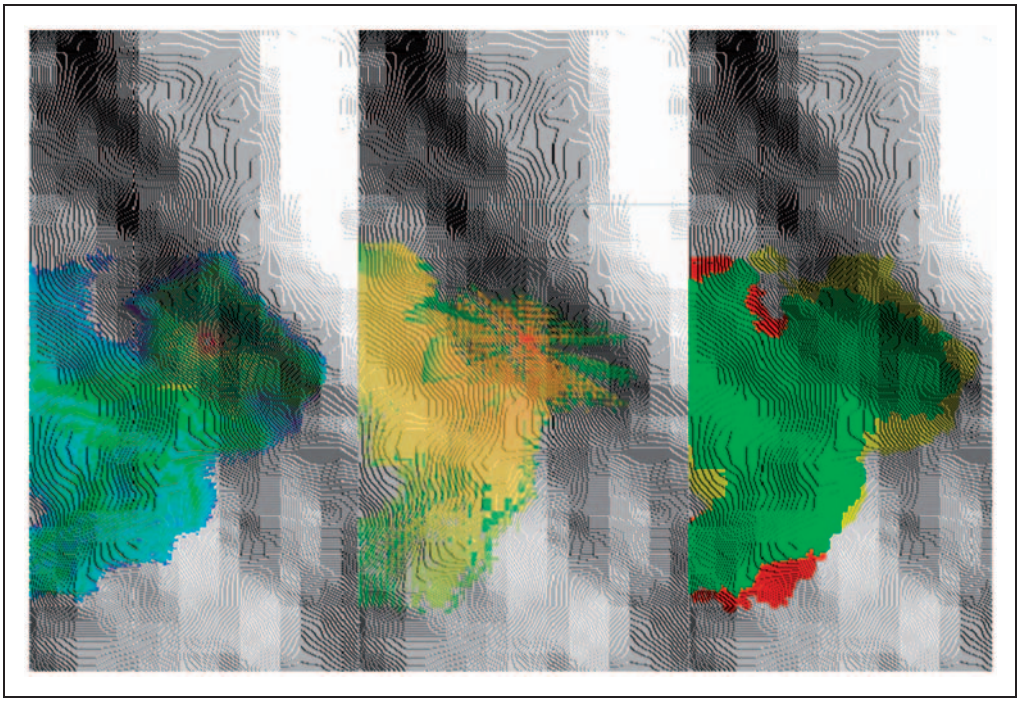

Figure 5. Radio coverage of the interference range of an example node for a given terrain using the Longley–Rice model (left), Durkin's model (middle), and their differences (right).

uses the threshold for interference. The right-most part of Figure 5 presents the difference in radio coverage (green color represents match, yellow is additional coverage given by the ITM model, while red is additional coverage given by Durkin's model).

It can be seen that the ITM model favors steeper areas, unlike Durkin's model, which is known to be pessimistic in similar cases. In addition, on the other hand, Durkin's model favors coverage of more distant points due to the single knife-edge diffraction. Overall, for all of the terrains studied, our analysis shows that the difference in radio coverage of the two models differs in only 20% of the coverage area in total, and these differences can only be found on the edges of the coverage area. The Durkin model provides radio coverage where, according to the ITM model there is none (red color in Figure 5), on 6% of the total radio-coverage area, while the ITM model provides radio coverage where Durkin's model does not (yellow color in Figure 5), on 14% of the total radio-coverage area. Of course, we cannot expect a complete match of the two areas since the two models are based on different principles. In addition, the comparison of several radio-propagation models made using real measured data,[32] clearly shows that the ITM model over-predicts path loss compared to Durkin's model that, on the other hand, under-predicts path loss. This behavior is especially the case for no-LOS links. The characteristic case shown in Figure 5 demonstrates matched findings. Since our implementation is a first-order approximation that uses only a single knife-edge diffraction, we believe that our further improvement of the model with multiple knife-edge diffractions will make the model even more realistic.

5. Simulation scenarios

The first set of results was made as a comparison of Durkin's model, with a regular flat terrain and the two-ray ground-propagation model in order to be able to compare the time of execution of the simulation scenarios and the results obtained for the same environment.

The second set of simulations is made to give some insight on the results that are to be expected when using Durkin's extension for realistic terrains. We chose two realistic terrains (see Figure 6 and Figure 7) from the vicinity of Eldorado. The maximum difference in elevations for both terrains is 200 m. We used random node mobility and random traffic.

For all simulation scenarios in the paper, we have 100 static nodes that are uniformly dispersed in the simulation area. As described above, the node transmission range is set to the standard 250 m given by the IEEE 802.11b standard wireless equipment. The antenna height is set to 1.5 m, and it has no relative offset against

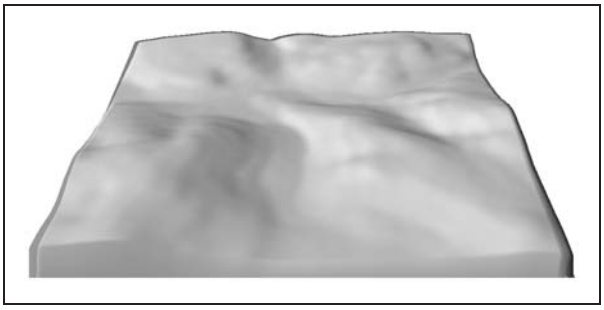

Figure 6. Real-terrain example 1 (1000 × 1000 m).

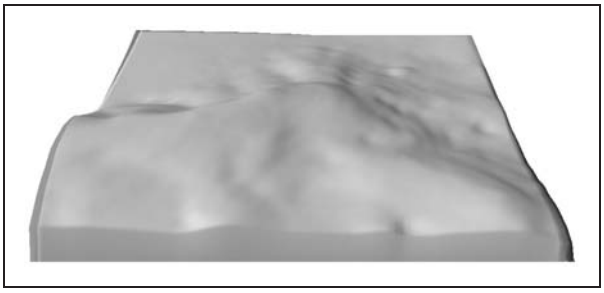

Figure 7. Real-terrain example 2 (1000 × 1000 m).

the wireless node. The offered network load is varied from 0.1 to 7 Mbps using User Datagram Protocol (UDP) data packets with 1 kB size. The simulation time is set to 1.5 hours, the average battery life of a notebook. We are utilizing the AODV (Ad Hoc On-Demand Distance Vector) protocol[33] for route discovery and path set up as well as the UDP protocol for data packets sending so that we do not have to deal with the Transmission Control Protocol (TCP) overhead.

In Figure 8, the network performances in terms of end-to-end throughput for two different node speeds are shown for the real-example terrains compared to the results obtained for a flat terrain using the two-ray ground model. It can easily be concluded that the terrain has a great impact on the network performances, and that it can also serve as a performance booster. Both of the terrains are narrowing down the interference range of the nodes, thus improving the rate of communications of closely positioned nodes. In this way, the overall performances of the network are enhanced. In Figure 9, a comparison of the time needed for execution of the simulation scripts for a scenario with real terrain and with no terrain data is given. As the offered load in the network raises, the execution time for real terrain data is lengthier since it mainly depends on the number of times each nodes tries to access the wireless medium in order to transmit a frame. However, even for offered load of 7 Mbps the execution time needed for simulations with real terrain

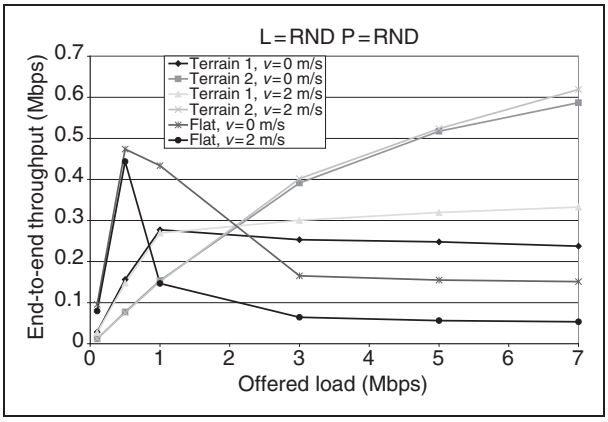

Figure 8. Network performances for two example real terrains compared to the flat-terrain approach.

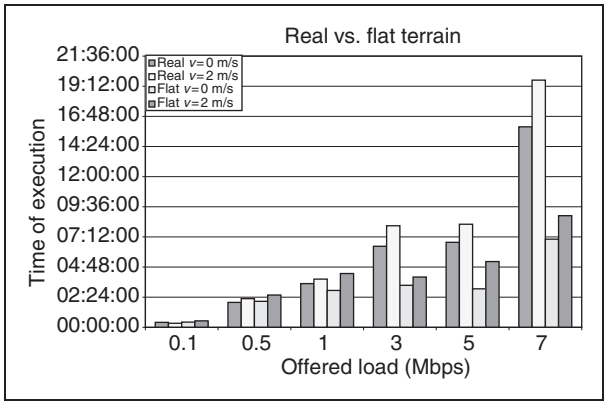

Figure 9. Comparison of time of execution for the real terrain example 1 and the flat-terrain approach.

data is less than 2 times over the time needed for flat-terrain simulations.

5.1. Case-study simulation environment

The common thread of all *ad hoc* network application themes is the human factor, i.e. the users that utilize the network for information sharing.[34] The social behavior directly affects the *ad hoc* network because we can easily associate the wireless mobile nodes with the social actors. The needs and affinities of the network user motivate the main goal of the *ad hoc* network node, including the physical positioning and the communication (logical) pattern.[35] In order to create a realistic model of the *ad hoc* network, we must have means to describe the relationship between the network users.

In the past decade, there have been several major findings that grasp the modeling and properties of social networks. The most influencing ones are the emergency of the small-world effect[36] and the scale-free property,[37] both of which can be found in every social network. The role of the small-world effect is to emphasize the natural grouping into communities, while the aim of the scale-free property is to create a situation for emergence of the rich-getting-richer phenomenon that models the tendency for a small number of individuals having a surprisingly high connectivity.[38] In order to bring the *ad hoc* communication modeling closer to a real-life situation by means of using the underlying social network of *ad hoc* users, we use a previously developed complex network model that captures the small-world and the scale-free phenomena in a way that the graph that corresponds to the user interaction is a blend of scale-free communities,[39] providing an uneven traffic distribution and a clustering effect in the network.

When analyzing an *ad hoc* network, the traffic-communication pattern is only one point where care must be taken that the modeling is suitably done. Furthermore, if we consider the social aspects of the *ad hoc* network users, we naturally expect the users to have a pattern of movement that will correspond to their social interconnections, that is, users that belong to the same community are expected to be in physical proximity of each other. In order to reflect this sort of behavior in our *ad hoc* network modeling, instead of standard random direction mobility generators, we use a modification of the community movement generator[40] in a way that allows us to simulate the movements of the scale-free communities obtained with our complex network model.

The primary objective of our case-study simulations is to understand the impact of the terrain presence in a simulation environment for *ad hoc* networks with communities. To this end, we evaluate the aspects of traffic throughput of Durkin's propagation model compared with the traditional flat-terrain approach. For the case-study evaluations made in this paper, we decided to work with fairly simple artificial terrains in the shape of a hillside, hill, ravine, and pyramid. In Figure 10, the terrain shapes are shown using the DEM file visualizing software 3Dem.[41] For comparison and verification purposes, we use the results obtained for a perfectly flat terrain. In this way, we can determine the impact of the terrain features on the network performances.

The created DEM files we used for the simulations were made with dimensions 10.000×10.000 m, with a 10:10:0.1 resolution. We used the scaling feature we implemented in the NS-2 simulator in order to obtain a precision of 1 m. Thus, the simulation area for all terrains is 1000×1000 m, with the highest point of 200 m.

The social community aspect of the network is implemented using the scale-free community model (S-FC). The node social behavior is implemented on two levels independently, logical and physical. The friend-to-friend communication is introduced via the scale-free community application layer.[39] The complete

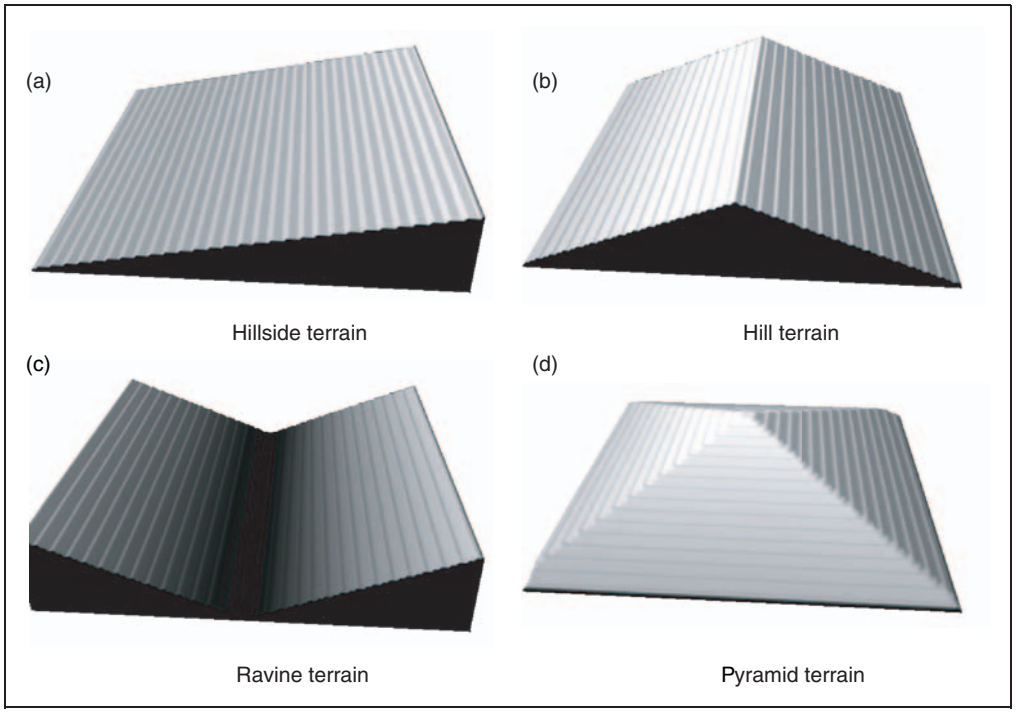

Figure 10. Terrains generated with our terrain generator that are going to be used for *ad hoc* network community performance analysis.

ad hoc network of 100 nodes is logically represented with four scale-free communities, each containing 25 nodes. The inter-community links are obtained using the originating hubs parameter set to 1 in order to obtain a representative social network that will have general characteristics that are close to real-life situations.[2] In this way, the traffic pattern in the network is following the social rules that imply frequent communication between friends from the same community, higher number of packets sent to the group leaders (hubs with a large number of social links) and inter-community data exchange using the group leaders.

As for the physical positioning of the nodes, we use a modified version of the social mobility model.[39] The generator is modified so that it reads in the generated scale-free community social network and then assigns proportional parts of the simulation area to each community. The nodes are uniformly scattered in the appropriate community area. During the simulation, the nodes are moving according to the random-direction model in the boundaries of their respective community. The average node speed is varied from 0 (static nodes) to 1, 2 or 5 m/s, with a deviation of 0.1 m/s.

Please note that the grouping on the physical level corresponds to the grouping on logical level, namely, we have the same four groups of nodes. The square XY projection of the terrain is divided into four identical square parts of size 500×500 m. Each *ad hoc* community has its own terrain part of the simulated area, and the nodes that belong to the group are uniformly scattered in their belonging area part.

Consequently, from the social community perspective, we have four different simulation settings, which are:

- L = RND, P = RND – no communities on application layer and no communities on physical layer; the nodes are randomly scattered in the whole area and the communication is completely randomized; this is the traditional approach when considering the network behavior and we use it for comparison.
- L = S-FC, P = RND – communities on application layer only; the nodes are randomly scattered in the whole area, but the communication is according the scale-free community social network.
- L = RND, P = S-FC – communities on physical layer only; the nodes are divided into four communities, but the communication pattern is completely random.
- L = SF-C, P = SF-C – communities on both application and physical layer; the nodes are physically dived into four communities and the communication pattern is according to the scale-free community social network. Take into consideration that these two types of communities (application and physical) are overlapping as this is the most expected case.

In order to make the necessary set of simulations for our observations of the relationship between the two-ray ground and Durkin's models, as well as for the relationship between the influence of the terrain and the communities on the network performances with nodes that move with different node speeds, the number of distinct simulations that need to be run is close to 600 for only one iteration. When striving to obtain average results from multiple runs, the number rises up to 6000. Given that the time for execution of one heavy load simulation is 5 to 7 hours, the time needed to make the necessary simulations starts to be measured in terms of months. In order to speed up the process, we decided to move the NS-2 code to our local branch of the SEEGRID infrastructure.[42] In this way, our simulation time execution became more than 20 times faster. At the same time, the easy way of defining all of the simulations at once and letting the grid manager worry about scheduling allows for efficient time fulfillment while waiting for the information that the jobs are done.

The parallel execution of multiple simulation scripts is a way for receiving results much more rapidly, and it is our strong belief that one should use this type of simulation execution as much as possible. Today's advances in technology allow for the creation of certain types of 'miniature' grids inside the personal computer using the various processor types available. One of our future works is to try to develop a parallel execution environment using all of the resources available on a given personal computer.

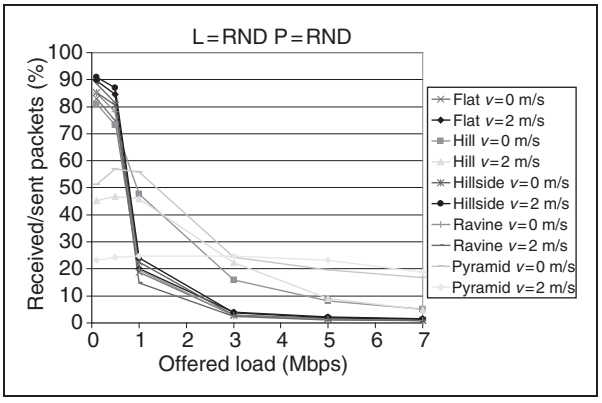

Figure 11. *Ad hoc* network performances for different terrains when using random mobility and traffic scenarios.

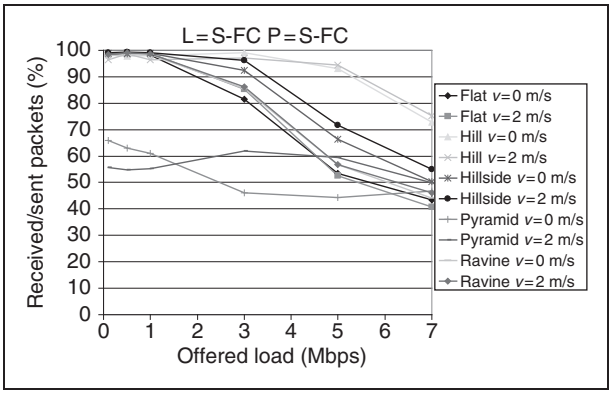

Figure 12. Performances of *ad hoc* network communities for different terrains.

6. Performance analysis of *ad hoc* network communities

One of the goals of this case study is to investigate the joint impact of the terrain features and node speed on the *ad hoc* network performances while introducing communities onto different layers in the network. For these purposes, we executed a number of simulation scenarios for different terrains, node speeds, and offered load, and measured the network performances in terms of end-to-end throughput (total Mbps received by all network nodes) and via the ratio of received and sent packets in the network.

In Figure 11, the obtained network performances for the different terrains and node speeds of 0 and 2 m/s are shown when using traditional network modeling using random mobility pattern and random traffic. It is clearly shown that once the offered load is above 1 Mbps, the received packets are a maximum of 25% of the sent, and this is only the case for the best scenario when the nodes are positioned on a pyramid terrain. The second-best scenario is for the hill terrain, while the rest show close values. The pyramid and the hill terrains exhibit better performances because of the possibilities for natural grouping of the nodes into two communities for the case of the hill and four communities for the case of the pyramid, while each community is placed on one slope of the terrain. This formation consequently lessens the interference between the nodes, and more parallel communications can be established simultaneously.

On the other hand, in Figure 12, the network nodes are grouped into physical and logical scale-free communities. The first obvious difference compared to Figure 11 is the 45% of received nodes that can be maintained for any offered load. Here, the hill shows the highest performances due to the overlapping of the natural and defined physical grouping of the nodes. As for the pyramid, one can notice that, in this case, although the performances are shown to be higher for higher loads in the network, the behavior of the network is deteriorated compared to the random case. This is a consequence of the badly chosen physical community placement compared to the natural terrain characteristics. Thus, one community can be found on

two sides of the pyramid, and the nodes that are cut from their group leader will suffer from signal blockage therefore experiencing low performances.

In order to conclude in what way the different types of communities (logical and physical) are influencing the network performances, in Figure 13 and Figure 14, we give results for the network performances obtained for offered loads of 3 Mbps when the communities in the network are modeled only on the physical level (Figure 13) and only on the logical level (Figure14) for different node speed.

When considering communities on a physical level only while the traffic is completely random (Figure 13), the results show somewhat better performances compared to the L = RND P = RND scenario without communities, especially for the cases of the hill and pyramid terrain since, in these cases, the communities are in accordance with the terrain features. The hillside also shows better performance than the flat terrain, but for smaller network loads; in the case of higher loads (as in the figure), the performances fall to the ones obtained for flat terrain. The ravine has the lowest performances because, in this case, the terrain features add to the possibility of interference.

The logical division into communities has a much bigger impact on the network performances, as can be concluded from the results presented in Figure 14. The performances are higher for all types of terrain, and are somewhat lower for the pyramid because of the problem with the group leaders that was described above. The results clearly show that the social community traffic modeling has the main lead in the performance outcome, especially when it is supported by an appropriate mobility pattern, Figure 15.

This conclusion can also be supported with the results shown in Figure 15, where the performances of a network modeled with different logical and physical layers are given for node speeds of 1 m/s and offered load of 3 Mbps. It is clear that the scale-free communities on both levels show outstanding performances, reaching up to 2.8 Mbps for the hill terrain compared to 0.6 Mbps for the completely random scenario. In Figure 16, a comparison is made for the results obtained with the different modeling choices and

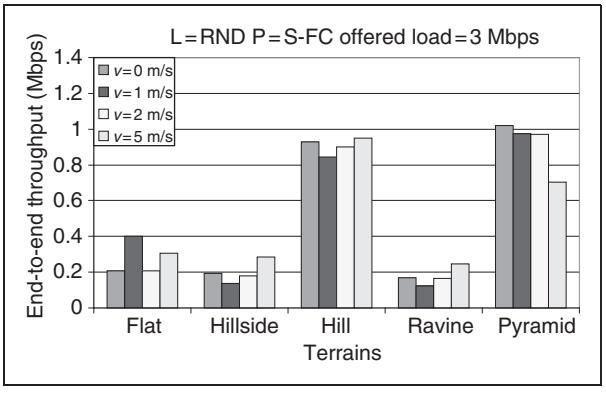

Figure 13. Terrain and speed impact on performances of *ad hoc* networks with physical communities.

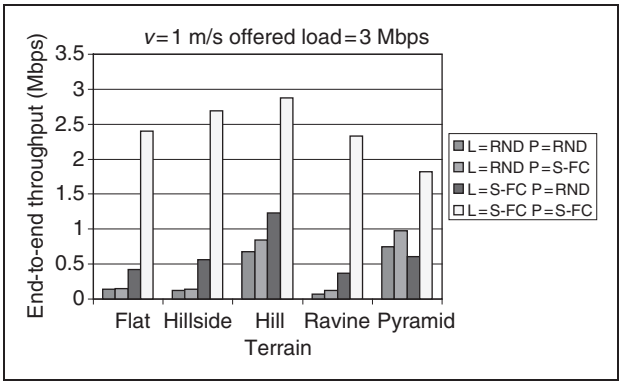

Figure 15. Impact of node communities on physical and logical level on the network performances for different terrains.

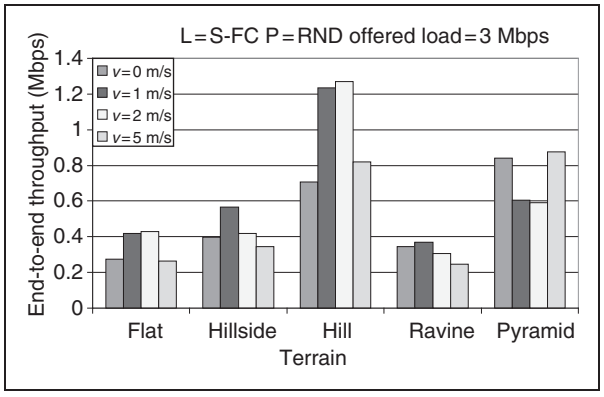

Figure 14. Terrain and speed impact on performances of *ad hoc* networks with logical communities.

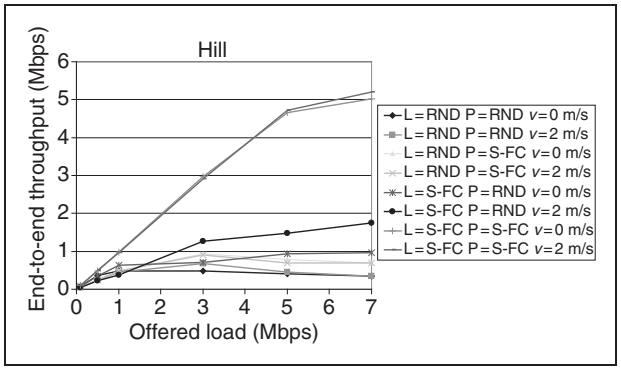

Figure 16. Impact of node communities on physical and logical level on the network performances for different node speeds on the hill terrain.

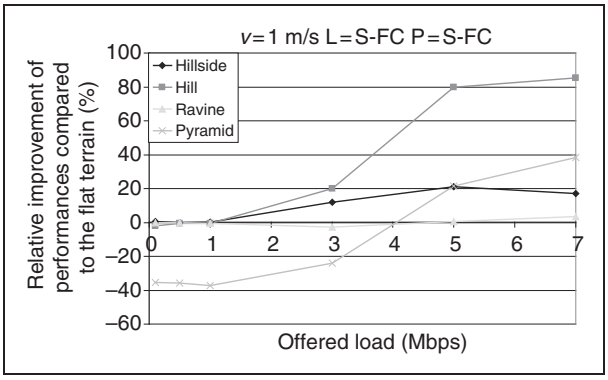

Figure 17. Relative improvement of the network community performances in a given terrain area when compared to the flat-terrain results.

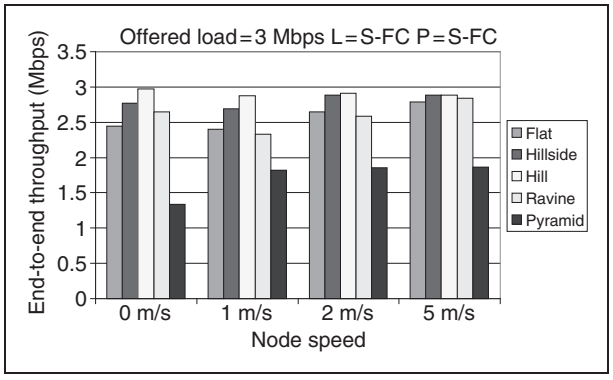

Figure 18. Impact of the terrain shape on the *ad hoc* network community performances for node speeds.

different node speeds for the 'best performing' terrain, i.e. the hill terrain. It can be seen that the L = S-FC P = S-FC scenario clearly outperforms the others for all types of network loads, rising up to 5 Mbps for high network loads, which is many times better compared to the best 1.8 Mbps given by the logical community only scenario.

The last two figures represent the impact of the terrain shape (Figure 17) and the node speed (Figure 18) on the best-performing scenario modeling, which includes scale-free communities on both logical and physical level.

Figure 17 presents the relative improvement in performances when the scenarios are conducted on a given terrain compared to the results obtained for the flat. These relative performances are calculated according to the following relation

$$\text{Rel.Performance} = \frac{\text{End2EndThroughput}_{\text{terrain}} - \text{End2EndThroughput}_{\text{FLAT}}}{\text{End2EndThroughput}_{\text{FLAT}}}. \quad (4)$$

It is interesting to note that, for small network loads, the network performances are almost the same with the flat, but as the load increases, the terrain features start to affect the outcome. In addition, it can be seen that for high-network loads, the terrains, except for the ravine, of course, add to the improvement of the performances of the network due to their shape. The most interesting case is the pyramid that, given the different network load, can give performances that differ from the one obtained for the flat terrain, from –40% up to +40%. This is caused by the fact that when the load is rising, there are more packets sent by the nodes, so the percentage lost because of the inconvenient node placement lessens.

Figure 18 presents the impact of the node speed in these types of scenarios. The network behavior of the increasing performances with node movement is not too moderate (as for the case with 5 m/s), and is preserved over the different terrains. It can also be seen that, as the node speed rises, the difference induced by the terrain shape reduces, except for the case of the pyramid, which has a somewhat much more different shape than the other example terrains.

From all of these observations, we can conclude that the terrain shape has great impact on the *ad hoc* network performances in all observed scenarios. When the network communities coincide with the separation of the nodes in terms of LOS induced by the terrain shape, we can expect performance improvements on a larger scale since the radio communication in the vicinity does not interfere with the one inside the cluster. In addition, for terrains with a rising complexity, the obtained results greatly differ in both values and shapes of the functions when compared to the ones obtained for a flat terrain. This clearly shows the importance of taking the terrain into consideration when discussing the *ad hoc* network performances.

7. Conclusion

Durkin's method is very attractive because it can read in a DEM and perform a site-specific propagation computation on the elevation data. It can produce results that are reported to be good within a few dB. Thus, these values are very good for our first-order observation of some large-scale factors that influence the *ad hoc* network performances. The disadvantages are that it cannot adequately predict propagation effects due to foliage, buildings, other fabricated structures, and it does not account for multipath propagation other than ground reflection, so additional loss factors are often included. The propagation phenomenon that is

modeled is LOS and diffraction from obstacles along the radial, and excludes reflections from other surrounding objects and local caterers. The effect of this assumption is that the model is somewhat pessimistic in narrow valleys, although it identifies isolated weak-reception areas rather well.

In this paper, an optimized version of the extension of the NS-2 simulator for using 3D terrain data in order to get more realistic results is introduced. The improved version is shown to introduce less than 20% execution time overhead when compared to the two-ray ground-propagation model. However, we find that this amount is more than tolerable when considering that the utilization of Durkin's propagation model bring us a large step closer to a more realistic environment.

Another attempt to observe the *ad hoc* networks in a more realistic environment is our case study of modeling of the social aspect of the network on both a logical and a physical level. This is done using the scale-free community model, which reflects the uneven distribution of traffic between the nodes and the natural occurrence of grouping in the network.

When investigating the performances of *ad hoc* network communities, our results show that, under certain terrain conditions, the terrain can play a major role in lowering, but also boosting, the *ad hoc* network performances. These results show that the presumption that the terrain will always impact on the performances towards its reduction is not always true. Thus, the terrain configuration must be taken into consideration and, if the situation allows, it may be used to improve the network performances, especially using the awareness of the natural community forming in the network on both, logical and physical levels.

The Durkin propagation model extension for the NS-2 is available for free use, and can be downloaded from http://e-tech.etf.ukim.edu.mk/e-tech/Research/3DpropagationextensionforNS2/tabid/107/Default.aspx.

References

1. Hekmat R. *Ad-hoc networks: fundamental properties and network topologies*. Netherlands: Springer, 2006.
2. Brown JS, Duguid P. *Social life of information*. Boston, Massachusetts: Harvard Business School Press, 2000.
3. Tonguz OK, Ferrari G. *Ad hoc wireless networks: a communication-theoretic perspective*. England: John Wiley & Sons, 2006.
4. Kumar ABR, Reddy LC and Hiremath PS. Performance comparison of wireless mobile ad-hoc network routing protocols. *International Journal of Computer Science and Network Security* 2008; Vol. 8, No. 6, pp. 337–343.
5. Lee CM, Pappas V, Sahu S, Seshan S. Impact of coverage on the performance of wireless ad hoc networks. *Proceedings of the Second Annual Conference of the International Technology Alliance,* London, UK, September 2008.
6. Shan W, Jian-xin W, Xu-dong Z, Ji-bo W. Performance of anti-jamming ad hoc networks using directional beams with group mobility. *IFIP International Conference on Wireless and Optical Communications Networks,* p.11–13, April 2006.
7. Baumann R, Heimlicher S, May M. Towards realistic mobility models for vehicular ad-hoc networks. *26th Annual IEEE Conference on Computer Communications IEEE INFOCOM 2007,* Alaska, USA, p.6–12, May 2007.
8. Edwards R and Durkin J. Computer prediction of service area for VHF mobile radio networks. *Proc IEEE 1969* 116: 1493–1500.
9. NS-2 network simulator, Available from: http://nsnam.isi.edu/nsnam/index.php.
10. Vuyyuru R, Oguchi K. Vehicle-to- vehicle ad hoc communication protocol evaluation using realistic simulation framework. *Fourth Annual Conference on Wireless on Demand Network Systems and Services, WONS '07,* 2007.
11. Gunes M and Wenig M. On the way to a more realistic simulation environment for mobile ad-hoc networks. *International Workshop on Mobile Services and Personalized Environments, GI LNI.* Germany, 2006.
12. Jardosh AP, Belding-Royer EM, Almeroth KC and Suri S. Real-world environment models for mobile network evaluation. *IEEE Journal on Selected Areas in Communications* 2005; 23: 622–632.
13. Harouna Souley A-k, Cherkaoui S. Realistic urban scenarios simulation for ad hoc networks. *Second International Conference on Innovations in Information Technology (IIT'05)*. Dubai, UAE, 2005.
14. Glomosim 'Global Mobile Information Systems Simulation Library', Available from: http://pcl.cs.ucla.edu/projects/glomosim/
15. OPNET Modeler Wireless Suite, Available from: http://www.opnet.com/solutions/network_rd/modeler_wireless.html.
16. George Hufford 'The ITS Irregular Terrain Model', Available from: http://flattop.its.bldrdoc.gov/itm.html.
17. 'TIREM Specifications', Available from: http://www.alionscience.com/index.cfm?fuseaction=Products.viewpage&productid=19&pageid=35.
18. Cost 231 Walfisch–Ikegami, 'Cost Final Report', Available from: http://www.lx.it.pt/cost231/.
19. 'The Guide to Geographic Information System', Available from: http://www.gis.com.
20. Harmon JE, Anderson SJ. *The design and implementation of geographic information systems*. New Jersey, USA: John Wiley & Sons, 2003.
21. US Geological Survey National Mapping Division, 'Part 1 General, Standards for Digital Elevation Models' U.S. Department of the Interior, U.S. Geological Survey, Reston, VA, USA, 2005.
22. US Geological Survey National Mapping Division, 'Part 2 Specifications, Standards for Digital Elevation Models' U.S. Department of the Interior, U.S. Geological Survey, Reston, VA, USA, 2005.
23. 'Terraform', Available from: http://firedrake.org/terraform/

24. 'Terragen', Available from: http://www.planetside.co.uk/terragen/
25. Rappaport TS. *Wireless communications: principles and practice*. New York, NY: Prentice Hall, 2002.
26. Lee WCY. *Mobile communications engineering*. New York, NY: McGraw Hill Publications, 1985.
27. Dadson CE, Durkin J and Martin E. Computer prediction of field strength in the planning of radio systems. *IEEE Transactions on Vehicular Technology* 1975; VT-24: 1–7.
28. Epstein D and Peterson DW. An experimental study of wave propagation at 840M/C. *Proceedings of IRE* 1953; 41: 595–611.
29. Wang Y. *A tutorial of 802.11 Implementation in NS-2*. MobiTec Lab: CUHK, Hong Kong, 2007.
30. Filiposka S, Trajanov D, Vuckovic M. Performances of clustered ad hoc networks on 3D terrains. *Second International Conference on Simulation Tools and Techniques SimuTOOLS'09,* Rome, Italy, March 2009, p.2–6.
31. 'Radio Mobile', Available from: http://www.cplus.org/rmw/english1.html.
32. Anderson H. New 2D physical EM propagation model selected. *IEEE Vehicular Technology Society News* 1997.
33. Perkins C. *Ad hoc on-demand distance vector (AODV) routing*. Internet-Draft Experimental RFC 3561, July 2003.
34. Rheingold H. *Smart mobs: the next social revolution*. Perseus book group, USA: Macquarie University, 2002.
35. Filiposka S, Trajanov D, Grnarov A. *Survey of social networking and applications in ad hoc networks*. Macedonia: National Conference on Electronics, Telecommunications, Automatics and Informatics, ETAI, 2007.
36. Watts DJ. *Six degrees: the science of a connected age*. New York, NY: W.W. Norton & Company, 2003.
37. Barabasi A-l. *Linked*. London: Penguin Group, 2003.
38. Gladwell M. *The tipping point*. New York, NY: Little, Brown, 2000.
39. Filiposka S, Trajanov D, Grnarov A. Performance analysis of scale-free communities in ad hoc networks. *IEEE WirelessVITAE'09*, Aalborg, Denmark, 17–20 May 2009.
40. Musolesi M, Mascolo C. A community based mobility model for ad hoc network research. *Proceedings 2nd ACM/SIGMOBILE International Workshop REALMAN'06*. Italy, 2006.
41. '3DEM', Available from: http://gisremote.blogspot.com/2008/02/3dem-software-ver-203-and-download.html.
42. 'South Eastern European Grid Enabled Infrastructure Development', Available from: http://www.see-grid.org/

Sonja Filiposka is an associate professor at the Faculty of Electrical Engineering and Information Technologies, Department of Computer Science, Skopje, FYR Macedonia.

Dimitar Trajanov is an associate professor at the Faculty of Electrical Engineering and Information Technologies, Department of Computer Science, Skopje, FYR Macedonia.